

Learning Relevant Contextual Variables Within Bayesian Optimization

Julien Martinelli^{*1} Ayush Bharti² Armi Tiihonen³ S. T. John² Louis Filstroff⁴ Sabina J. Sloman⁵
Patrick Rinke³ Samuel Kaski^{2,5}

¹Inserm Bordeaux Population Health, Vaccine Research Institute, Université de Bordeaux, Inria Bordeaux Sud-ouest, France

²Department of Computer Science, Aalto University, Helsinki, Finland

³Department of Applied Physics, Aalto University, Helsinki, Finland

⁴Univ. Lille, CNRS, Centrale Lille, UMR 9189 CRISTAL, F-59000 Lille, France

⁵Department of Computer Science, University of Manchester, Manchester, United Kingdom

Abstract

Contextual Bayesian Optimization (CBO) efficiently optimizes black-box functions with respect to design variables, while simultaneously integrating *contextual* information regarding the environment, such as experimental conditions. However, the relevance of contextual variables is not necessarily known beforehand. Moreover, contextual variables can sometimes be optimized themselves at an additional cost, a setting overlooked by current CBO algorithms. Cost-sensitive CBO would simply include optimizable contextual variables as part of the design variables based on their cost. Instead, we adaptively select a subset of contextual variables to include in the optimization, based on the trade-off between their *relevance* and the additional cost incurred by optimizing them compared to leaving them to be determined by the environment. We learn the relevance of contextual variables by sensitivity analysis of the posterior surrogate model while minimizing the cost of optimization by leveraging recent developments on early stopping for BO. We empirically evaluate our proposed Sensitivity-Analysis-Driven Contextual BO (SADCBO) method against alternatives on both synthetic and real-world experiments, together with extensive ablation studies, and demonstrate a consistent improvement across examples.

1 INTRODUCTION

Bayesian optimization (BO) is a sample-efficient black-box optimization method, typically used when the objective function is too expensive to optimize directly [Garnett, 2023]. Given an objective function that can be evaluated pointwise over a set of *design variables*, BO combines surrogate mod-

eling with a pre-specified policy of evaluation over the design space (the so-called acquisition function) to efficiently locate the global optimum of the function. BO has been especially useful in automatic discovery of materials [Zhang et al., 2020], molecules [Fang et al., 2021], and pharmaceutical compounds [Gómez-Bombarelli et al., 2018, Korovina et al., 2020]—problem domains in which evaluating the performance of a candidate depends on a costly experiment.

Despite the success of BO and its recent algorithmic advancements, open challenges remain for its practical use. A key implicit assumption in vanilla BO is that the objective function only depends on the design variables. This assumption is violated in many practical scenarios, wherein various *uncontrolled* environmental factors and experimental settings, referred to as *contextual variables* [Krause and Ong, 2011, Kirschner et al., 2020, Arsenyan et al., 2023], also affect the objective function. For instance, ambient humidity was found to influence the experiments in robot-assisted material design [Nega et al., 2021], such that the best compound differed with humidity conditions. Moreover, in practice, the domain experts themselves might not know *a priori* which contextual variables are relevant, and would observe their confounding effect only during the course of the optimization process. Therefore, it is critical to identify the contextual variables that significantly affect the objective function, not only to achieve the highest optimization results, but also for the practitioners to reliably reproduce experimental results.

To deal with the uncertainty related to the contextual variables, variants of BO have been developed. In particular, Krause and Ong [2011] introduced the Contextual Bayesian optimization (CBO) framework, which uses the uncontrollable contextual information known *before* the experiment, like current environmental conditions, to enhance the surrogate model. Alternatively, several works have proposed to alter the simple optimization objective to make it robust in some sense, such as by taking the expectation with respect to the contextual variables [Toscano-Palmerin and Frazier, 2022], or considering distributionally-robust scenar-

^{*}Work done while at Aalto University.

ios [Bogunovic et al., 2018, Kirschner et al., 2020]. However, these works consider a different setup than the original CBO framework, as contextual information is only revealed *after* the design has been sent for experiment, not before. Besides this distinction, in some applications, contextual variables *can* be controlled, and therefore set to values they may be unlikely to take during passing observation. Such variables are, for instance, synthesis conditions of material samples, including sintering temperature or the used solvents. Certain environmental conditions like room temperature or ambient humidity are also “principally” controllable during the course of an experiment [Higgins et al., 2021, Nega et al., 2021]. Nevertheless, whether their inclusion as optimization variables is relevant or not may not be straightforward to predict [Abolhasani and Brown, 2023]. Moreover, optimizing over all the potentially relevant contextual variables can improve BO performance, but this process can be costly, thus invoking a cost-versus-efficiency trade-off.

Contributions. In this paper, we extend the CBO framework to settings in which the relevance of contextual variables is (i) not known beforehand, and (ii) can be optimized, but at some cost. We propose a Sensitivity-Analysis-Driven CBO (SADCBO) algorithm for the simultaneous identification and optimization of relevant contextual variables. SADCBO leverages recent advances in sensitivity-analysis-driven variable selection [Sebenius et al., 2022] and early stopping criteria for BO [Ishibashi et al., 2023]. We emphasize that SADCBO combines the *contextual observational* setting, where the context information is only observed, and the *contextual optimization* setting, where contextual variables can be optimized (similar to design variables), into a sequential algorithm. In effect, SADCBO provides a way to navigate the following tradeoff: should contextual variables be taken *as is* at no cost, or should they be steered outside of their observational distribution in order to provide more information about the objective, at a cost? We evaluate the performance of SADCBO, comparing against methods from the CBO and high-dimensional BO literature, on both synthetic and real-world cases.

65

2 CONTEXTUAL BAYESIAN OPTIMIZATION (CBO)

66 The CBO framework [Krause and Ong, 2011] deals with
 67 a black-box function $f : \mathcal{X} \times \mathcal{Z} \rightarrow \mathbb{R}$ defined on the joint
 68 space of both the *design variables* $\mathcal{X} \subset \mathbb{R}^d$ and *contextual*
 69 *variables* $\mathcal{Z} \subset \mathbb{R}^c$. We assume that we get noisy evalua-
 70 tions of f , that is, we observe the output $y = f(\mathbf{x}, \mathbf{z}) + \varepsilon$
 71 with $\varepsilon \sim \mathcal{N}(0, \sigma_{\text{noise}}^2)$. A Gaussian process (GP) prior
 72 [Rasmussen and Williams, 2006] is placed on f ; with
 73 the notation $\mathbf{v} = [\mathbf{x}, \mathbf{z}]$, we write $f(\mathbf{v}) \sim \mathcal{GP}(0, k(\mathbf{v}, \mathbf{v}'))$.

A GP is a stochastic process fully characterized by its mean function (taken here to be zero) and its kernel $k(\mathbf{v}, \mathbf{v}') = \text{cov}[f(\mathbf{v}), f(\mathbf{v}')]$. This implies that for any finite-dimensional collection of inputs $[\mathbf{v}_1, \dots, \mathbf{v}_t]$, the function values $\mathbf{f} = [f(\mathbf{v}_1), \dots, f(\mathbf{v}_t)]^\top \in \mathbb{R}^t$ follow a multivariate normal distribution $\mathbf{f} \sim \mathcal{N}(\mathbf{0}, \mathbf{K})$, where $\mathbf{K} = (k(\mathbf{v}_i, \mathbf{v}_j))_{1 \leq i, j \leq t}$ is the kernel matrix. Given a dataset $\mathcal{D}_t = \{(\mathbf{x}_i, \mathbf{z}_i, y_i)\}_{i=1}^t = \{(\mathbf{v}_i, y_i)\}_{i=1}^t$, the posterior distribution of $f(\mathbf{v})$ given \mathcal{D}_t is Gaussian, with analytical expressions for the mean $\mu_t(\mathbf{v}|\mathcal{D}_t)$ and variance $\sigma_t^2(\mathbf{v}|\mathcal{D}_t)$.

In the CBO setting, we first observe the context variables, and then choose the design variables accordingly. More precisely, at iteration $t+1$, a context vector \mathbf{z}_{t+1} is observed, assumed to have been drawn from an unknown distribution $p(\mathbf{z})$, and the optimal design \mathbf{x}_{t+1}^* is such that

$$\mathbf{x}_{t+1}^* = \arg \max_{\mathbf{x} \in \mathcal{X}} f(\mathbf{x}, \mathbf{z}_{t+1}). \quad (1)$$

Given \mathbf{z}_{t+1} and the previous t observations \mathcal{D}_t , the next candidate design \mathbf{x}_{t+1} is selected using the Upper Confidence Bound (UCB) acquisition function α [Srinivas et al., 2012]:

$$\begin{aligned} \mathbf{x}_{t+1} &= \arg \max_{\mathbf{x} \in \mathcal{X}} \alpha(\mathbf{x}, \mathbf{z}_{t+1} | \mathcal{D}_t) \\ &= \mu_t(\mathbf{x}, \mathbf{z}_{t+1} | \mathcal{D}_t) + \beta_t^{1/2} \sigma_t(\mathbf{x}, \mathbf{z}_{t+1} | \mathcal{D}_t), \end{aligned} \quad (2)$$

for a sequence $(\beta_t)_{t \geq 1}$. This incurs a design cost $\lambda_{\mathbf{x}}$.

Extending the CBO problem setup. We extend the problem setting of CBO in two ways. Firstly, we assume that only a subset of the contextual variables truly affect f . Let $\mathbf{z} = [z^{(1)}, \dots, z^{(c)}]$ be the vector of all contextual variables. For any set J belonging to the power set of $\{1, \dots, c\}$, denote by $\mathbf{z}^{(J)} \in \mathbb{R}^{|J|}$ the vector of reduced dimension whose variables are indexed by J . For instance, if $J = \{1, 3\}$, then $\mathbf{z}^{(J)} = [z^{(1)}, z^{(3)}]$. We assume that there exists a set J^* , where $|J^*| \ll c$, such that $f(\mathbf{x}, \mathbf{z}) = f(\mathbf{x}, \mathbf{z}^{(J^*)}) \forall (\mathbf{x}, \mathbf{z})$. Secondly, we include the possibility of setting the value of any of the contextual variables at some cost over and above the usual design query cost $\lambda_{\mathbf{x}}$. This means that for all $j \in \{1, \dots, c\}$, the context variable $z^{(j)}$ can be optimized at a cost λ_j . To be able to control each contextual variable, we must also assume their independence: $p(\mathbf{z}) = \prod_{j=1}^c p(z^{(j)})$. With these additional assumptions, we aim to maximize the function f in a cost-efficient manner, while identifying the optimal set J^* . This provides the user with a comprehensive summary of the relevant contextual variables found through optimization, thus ensuring reproducibility and explainability. Unlike CBO, the ability to control contextual variables allows us to judge whether or not one should optimize contextual variables to learn more about the objective (albeit at a cost), or if the current sampled context is already informative enough. Specifically, we aim to maximize the objective

$$(\mathbf{x}_{t+1}^*, \mathbf{z}_{t+1}^*) = \arg \max_{(\mathbf{x}, \mathbf{z}_{t+1}^{(J^*)}) \in \mathcal{X} \times \prod_{j \in J^*} \mathcal{Z}_j} f(\mathbf{x}, \mathbf{z}_{t+1}) \quad (3)$$

116 where, for all $j \in J^*$, we optimize $z_{t+1}^{(j)}$ at cost λ_j , and all
 117 other elements $j' \in \{1, \dots, c\} \setminus J^*$ of \mathbf{z}_{t+1} remain at their
 118 values sampled from the environment ($z_{t+1}^{(j')} \sim p(z^{(j')})$).

3 METHODOLOGY

119 To solve the extended CBO problem introduced in Section 2,
 120 we identify relevant contextual variables, building on a vari-
 121 able selection technique from the GP literature [Sebenius
 122 et al., 2022]. Section 3.1 describes our adaptation of this
 123 method to the optimization setting, by restricting the dataset
 124 to high function values. Section 3.2 then presents our se-
 125 quential algorithm SADCBO, which employs the adapted
 126 variable selection method in solving the optimization prob-
 127 lem. A flowchart summarizing the proposed method can be
 128 found in Figure S1.

3.1 VARIABLE SELECTION FOR CBO VIA SENSITIVITY ANALYSIS

129 To handle the presence of contextual variables that can be
 130 optimized, one approach is to include them in the design
 131 space. However, such a strategy can be infeasible when their
 132 relevance is not known *a priori* and domain experts can only
 133 provide a candidate set of *potentially* relevant contextual
 134 variables. Indeed, this leads to an exponential expansion of
 135 the search space, while at the same time increasing the cost
 136 of optimization. In such cases, it is crucial to identify the
 137 *relevant* contextual variables, i.e., to find (a good approx-
 138 imation to) the optimal set J^* . This not only allows us to
 139 optimize the function more efficiently but also provides ad-
 140 ditional insights about the experiment to the domain experts.

141 To approximate the optimal set J^* , we include those context-
 142 ual variables that are most relevant for identifying the opti-
 143 mum, which we estimate using sensitivity analysis. Specifi-
 144 cally, we adapt the Feature Collapsing (FC) method [Sebe-
 145 nius et al., 2022]. The FC method perturbs training points
 146 (namely, by setting one feature to zero), and measures the
 147 induced shift in the posterior predictive distribution in terms
 148 of KL divergence. Given a dataset $\mathcal{D}_t = \{(\mathbf{x}_i, \mathbf{z}_i, y_i)\}_{i=1}^t$,
 149 the relevance $r_{i,j}$ on the i^{th} sample of the j^{th} contextual
 150 variable $z_i^{(j)}$ is computed as

$$r_{i,j} = \text{KL}(p(y_* | \mathbf{x}_i, \mathbf{z}_i, \mathcal{D}_t) || p(y_* | \mathbf{x}_i, \mathbf{z}_i \odot \xi[j], \mathcal{D}_t)), \quad (4)$$

151 where $\xi[j] = [\xi^{(1)}, \dots, \xi^{(c)}]$ is a vector so that $\xi^{(j)} =$
 152 0, and $\xi^{(j')} = 1$ for $j' \neq j$, and \odot is the element-wise
 153 multiplication. The relevance score of the j^{th} contextual
 154 variable is then computed as an average over \mathcal{D}_t :

$$\text{FC}_{\mathcal{D}_t}(j) = \frac{1}{|\mathcal{D}_t|} \sum_{i=1}^{|\mathcal{D}_t|} \left(\frac{r_{i,j}}{\sum_{j'=1}^c r_{i,j'}} \right). \quad (5)$$

155 The FC scores obtained in this manner reveal the variables
 156 that are relevant for predicting the output *across* \mathcal{D}_t . As our

goal is to *maximize* f , we are interested in identifying con-
 157 textual variables that are relevant for *high* function values.
 158 Hence, we adapt Equation (5) to the BO setting by modify-
 159 ing the dataset over which the scores are averaged. We use
 160 information about high function values from two different
 161 sets: (1) The subset \mathcal{D}^{γ_t} associated with the highest output
 162 values observed so far:

$$\mathcal{D}_t^{\gamma_t} = \{(\mathbf{x}_i, \mathbf{z}_i, y_i) \in \mathcal{D}_t \mid y_i / y_{\text{best}} \geq \gamma_t\}, \quad (6)$$

163 where $y_{\text{best}} = \max_{1 \leq i \leq t} y_i$ is the current observed maxi-
 164 mum. For example, using $\gamma_t = 0.8 \forall t$ would yield a $\mathcal{D}_t^{\gamma_t}$
 165 that consists of the highest 20% observations so far. (2) We
 166 select a batch of Q points $\mathcal{D}_t^Q := \{(\mathbf{x}_q^*, \mathbf{z}_{t+1})\}_{q=1}^Q$ that are
 167 promising given the next context \mathbf{z}_{t+1} :

$$\{\mathbf{x}_q^*\}_{q=1}^Q = \arg \max_{\{\mathbf{x}_q\}_{q=1}^Q \in \mathcal{X}^Q} \alpha^{\text{Batch}}(\{(\mathbf{x}_q, \mathbf{z}_{t+1})\}_{q=1}^Q \mid \mathcal{D}_t), \quad (7)$$

168 where α^{Batch} denotes a batched version of the acquisition
 169 function α such as Q -UCB for UCB [Wilson et al., 2017].
 170 We use the union $\mathcal{D}_t^{\text{BO}} = \mathcal{D}_t^{\gamma_t} \cup \mathcal{D}_t^Q$ as our dataset for FC.
 171 Therefore, we compute $\text{FC}_{\mathcal{D}_t^{\text{BO}}}$ based on Equation (5). The
 172 importance of working with $\mathcal{D}_t^{\text{BO}}$ instead of \mathcal{D}_t is illustrated
 173 in Figure 1 on a toy example.

174 We successively select the indices of the contextual variables
 175 with the highest FC scores until their cumulative FC score
 176 exceeds some chosen threshold $\eta \in [0, 1]$, meaning that the
 177 selected variables explain the fraction η of the output sensi-
 178 tivity amongst all contextual variables. Let J_η denote the set
 179 of indices of the selected contextual variables. We train a GP
 180 surrogate based on $\{(\mathbf{x}_i, \mathbf{z}_i^{(J_\eta)}, y_i)\}_{i=1}^t$ and can select a new
 181 design through maximization of the acquisition function α :

$$\mathbf{x}_{t+1} = \arg \max_{\mathbf{x} \in \mathcal{X}} \alpha(\mathbf{x}, \mathbf{z}_{t+1}^{(J_\eta)} \mid \mathcal{D}_t). \quad (8)$$

182 Note that other measures of variable relevance could have
 183 been used, e.g., the method proposed by Spagnol et al.
 184 [2019] based on maximum mean discrepancy [Gretton et al.,
 185 2012]. We found FC to perform better (see Section 5.2).

3.2 SENSITIVITY-ANALYSIS-DRIVEN CBO (SADCBO)

186 Building on top of the variable selection method discussed in
 187 Section 3.1, we now present SADCBO, a sequential method
 188 for performing BO in the presence of irrelevant contextual
 189 variables. SADCBO proceeds in two phases.

190 In the first, *observational* phase, we choose to only observe
 191 the values of the contextual variables without optimizing
 192 over them. This ensures that we do not waste budget op-
 193 timizing the contextual variables when their relevance is
 194 computed based on a limited amount of data, and hence
 195 can be noisy. We select the contextual variables based on
 196 their FC relevance and then use vanilla CBO as described

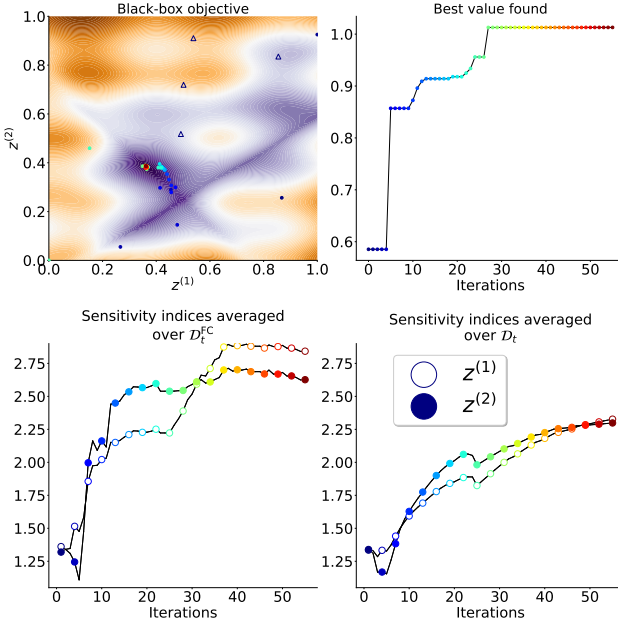


Figure 1: **Sensitivity analysis on $\mathcal{D}_t^{\text{BO}}$ characterizes variable importance at the optimum faster than \mathcal{D}_t .** Top left: 2D black-box objective together with the queries produced along a BO trajectory. Initial samples are represented by empty dark-colored triangles, newly obtained samples as dots with an increasingly lighter color. Top right: Best value found during the optimization trial. Bottom left: Sensitivity indices for $z^{(1)}$ and $z^{(2)}$ averaged over $\mathcal{D}_t^{\text{BO}}$. As we converge to the optimum, $\mathcal{D}_t^{\text{BO}}$ mainly involves samples close to the optimum, leading to a different variable relevance ranking (iteration 30 to the end; $z^{(1)}$ is more relevant) compared to the early iterations (10 to 30; $z^{(2)}$ is more relevant). Bottom right: Sensitivity indices computed on the whole dataset \mathcal{D}_t do not converge as quickly and do not capture the shift in relevance close to the optimum.

in Section 2 to optimize the design variables. Thus, in this phase, we leverage the available contextual information to guide design selection.

In the early stage of the optimization, cheap queries where contextual variables are not optimized still provide a considerable amount of information. The information gained from purely observing contextual variables will, however, saturate at some point, leading to diminishing simple regret differences. At this point, it becomes necessary to pay the higher price to control more dimensions of the input space. This motivates the introduction of a second phase, in which contextual variables can have their values arbitrarily set, through optimization.

In the second, contextual *optimization* phase, we optimize the contextual variables selected at each iteration based on their FC relevance. As optimizing a context variable $z^{(j)}$ is associated with a cost λ_j , we modify the FC relevance in

Equation (5):

$$\tilde{\text{FC}}_{\mathcal{D}_t}(j) = \text{FC}_{\mathcal{D}_t}(j)/\lambda_j \quad (9)$$

Our variable selection criterion can then be interpreted as the degree of sensitivity *per unit cost*. This allows SADCBO to automatically trade off a variable's potential to greatly affect the optimum with the associated optimization cost. As before, once the contextual variables $\mathbf{z}^{(J_\eta)}$ have been selected, we train a GP surrogate using $\{(\mathbf{x}_i, \mathbf{z}_i^{(J_\eta)}, y_i)\}_{i=1}^t$ and select the next design and contextual variables to query as

$$(\mathbf{x}_{t+1}, \mathbf{z}_{t+1}^{(J_\eta)}) = \arg \max_{(\mathbf{x}, \mathbf{z}^{(J_\eta)}) \in \mathcal{X} \times \prod_{j \in J_\eta} \mathcal{Z}_j} \alpha(\mathbf{x}, \mathbf{z}^{(J_\eta)} | \mathcal{D}_t). \quad (10)$$

In effect, J_η represents our approximation for J^* as introduced in Equation (3). Note that our acquisition function is not cost-weighted, as cost-weighted acquisition functions can dramatically underperform [Lee et al., 2021], specifically for non-continuous cost models. Including the cost at the model selection level avoids this issue.

Switching from observational to optimization phase. We employ the criterion proposed by Ishibashi et al. [2023] for determining the stopping time in BO. Using this criterion, we detect the point at which the optimization gain based on purely observing the contextual variables diminishes, following which the contextual optimization phase begins. We now briefly describe the details of this switching criterion.

With $\mathbf{v} = [\mathbf{x}, \mathbf{z}]$, let $\mathbf{v}_t^* = \arg \max_{\mathbf{v} \in \mathcal{D}_t} f(\mathbf{v})$ be the current best candidate point in the dataset up to time t . Denoting $f^* := \max_{\mathbf{v} \in \mathcal{V}} f(\mathbf{v})$, let $R_t = f^* - \mathbb{E}_{\hat{f} \sim p(f|\mathcal{D}_t)} [\max_{\mathbf{v} \in \mathcal{V}} \hat{f}(\mathbf{v})]$ be the expected minimum simple regret. Then, with probability $1 - \delta$, $\Delta R_t = |R_t - R_{t-1}|$ can be upper bounded by $\Delta \tilde{R}_t$ with

$$\begin{aligned} \Delta \tilde{R}_t &= v(\phi(g) + g\Phi(g)) + |\Delta \mu_t^*| \\ &\quad + \kappa_{\delta, t-1} \sqrt{\frac{1}{2} \text{KL}(p(f|\mathcal{D}_t) || p(f|\mathcal{D}_{t-1}))}, \end{aligned} \quad (11)$$

where $\phi(\cdot)$ and $\Phi(\cdot)$ are the p.d.f. and c.d.f. of a standard Gaussian distribution, respectively, $\Delta \mu_t^* := \mu_t(\mathbf{v}_t^*) - \mu_{t-1}(\mathbf{v}_{t-1}^*)$, $v := \sqrt{\sigma_t^2(\mathbf{v}_t^*) - 2\Sigma_t(\mathbf{v}_t^*, \mathbf{v}_{t-1}^*) + \sigma_{t-1}^2(\mathbf{v}_{t-1}^*)}$, $g := \Delta \mu_t^*/v$, and $\kappa_{\delta, t-1}$ is a sequence indexed by t and depending on δ . Then, we switch from the observational to the optimization phase in SADCBO when $\Delta \tilde{R}_t \leq s_t$, where

$$s_t := \frac{(\sigma_{t-1}(\mathbf{v}_t^*) + \kappa_{\delta, t-1}/2) \sigma_{t-1}(\mathbf{v}_t) \sigma_{\text{noise}} \sqrt{-2 \log \delta}}{\sigma_{t-1}^2(\mathbf{v}_t) + \sigma_{\text{noise}}^2}. \quad (12)$$

Further details about the derivation of s_t and the expression of $\kappa_{\delta, t-1}$ can be found in Appendix B. The entire algorithm is summarized in Algorithm 1.

Algorithm 1 SADCBO

1: **Input:** initial dataset \mathcal{D}_0 , hyperparameters η and γ ,
batch size Q , budget Λ , costs $\lambda_x, \lambda_1, \dots, \lambda_c$
2: Train initial GP using \mathcal{D}_0 and all variables $[\mathbf{x}, \mathbf{z}]$.
phase = observational. $t = 1$.
3: **while** $\Lambda \geq \lambda_x$ **do**
4: Receive context $\mathbf{z}_{t+1} \sim p(\mathbf{z})$
5: Assemble dataset $\mathcal{D}_t^{\text{BO}}$ (Equations (6) and (7))
6: Compute $\text{FC}_{\mathcal{D}_t^{\text{BO}}}(j)$ for all j (Equation (5) or (9) if
phase = optimization)
7: In descending order, add indices to J_η until
 $\sum_{j \in J_\eta} \text{FC}_{\mathcal{D}_t^{\text{BO}}}(j) > \eta$
8: Train lower-dimensional GP $\{(\mathbf{x}_i, \mathbf{z}_i^{(J_\eta)}, y_i)\}_{i=1}^t$
9: Get \mathbf{x}_{t+1} (Equation (8)) (and \mathbf{z}_{t+1} (Equation (10)) if
phase = optimization)
10: Acquire observation y_{t+1} at $[\mathbf{x}_{t+1}, \mathbf{z}_{t+1}]$
11: $\mathcal{D}_{t+1} \leftarrow \mathcal{D}_t \cup \{(\mathbf{x}_{t+1}, \mathbf{z}_{t+1}, y_{t+1})\}$
12: Retrain full GP
13: **if** phase = observational and $\Delta \tilde{R}_t \leq s_t$ [based on
 $p(f|\mathcal{D}_{t+1})]$ (Equation (12)) **then**
14: phase = optimization
15: **end if**
16: $\Lambda \leftarrow \Lambda - \lambda_x + \sum_{j \in J_\eta} \lambda_j$, $t \leftarrow t + 1$
17: **end while**

4 RELATED WORK

246 **Robust BO.** Bogunovic et al. [2018], Kirschner et al.
247 [2020], Husain et al. [2023] and Saday et al. [2023] perform
248 worst-case optimization under fluctuations of the contextual
249 variables. In particular, Distributionally-Robust BO [DRBO,
250 Kirschner et al., 2020] tries to maximize the expected black-
251 box function value under the worst-case distribution of the
252 contextual variables. This worst-case distribution belongs to
253 an ‘‘uncertainty set’’, a ball centered around a reference dis-
254 tribution that is gradually learned [Tulabandhula and Rudin,
255 2014]. However, as in Krause and Ong [2011], these works
256 assume that the relevant contextual variables are known *a*
257 *priori*, and can only be observed, *after the designs have*
258 *been selected*, and not controlled.

259 **High-dimensional BO.** Due to the curse of dimensionality,
260 the performance of standard BO is severely degraded
261 when applied in high-dimensional input spaces. To tackle
262 this problem, most approaches either aim at carrying out
263 BO in a lower-dimensional space instead of the original or
264 work with a structured GP surrogate. A lower-dimensional
265 subspace can be found in a data-agnostic manner, for
266 instance by randomly dropping dimensions of the problem [Li
267 et al., 2017] or considering tree-like random decomposi-
268 tions [Ziomek and Bou-Ammar, 2023]. Data-driven meth-
269 ods based on various measures of feature relevance have also
270 been proposed [Spagnol et al., 2019, Shen and Kingsford,
271 2021]. In contrast, structured surrogate methods encode

272 structural information about the objective, for instance us-
273 ing an additive kernel, yielding an acquisition function that
274 is additive under the provided decomposition [Rolland et al.,
275 2018]. Finally, Eriksson and Jankowiak [2021] and Liu et al.
276 [2023] proposed using a sparsity-enforcing GP surrogate,
277 equipped with a heavy-tailed horseshoe prior on the squared
278 inverse lengthscales.

279 **Cost-aware BO.** In most methods, the BO budget is given
280 in iterations, implicitly assuming that each evaluation has
281 the same cost. In practice, cost may vary significantly across
282 different regions of the input space [Lee et al., 2020], or
283 depend on the number of variables we optimize over. Cost-
284 aware BO integrates the cost-constrained nature of the prob-
285 lem, usually within the acquisition function. Let us also
286 mention more involved strategies like constrained Markov
287 decision processes when the total budget is known before-
288 hand [Lee et al., 2021]. The recent work by Tay et al. [2023]
289 carries out Robust BO while at the same time involving a
290 notion of controlled variables at a cost. However—unlike
291 our framework—they require the nonselected variables to
292 be sampled from a *known* distribution at each iteration.

5 EXPERIMENTAL RESULTS

293 We evaluate our approach on several real-world examples
294 and synthetic functions, described in Section 5.1. We com-
295 pare against multiple baselines (Table 1) and present results
296 in Section 5.2. In Section 5.3 we discuss the influence of vari-
297 ous experimental settings: number of noise variables present,
298 contextual variable query cost, surrogate and method hy-
299 perparameters. We conclude by presenting several insights
300 regarding the phase-switching criterion.

301 **Baselines.** We benchmark our approach, coined SADCBO,
302 against baselines referenced in Table 1. In particular, MMDBO
303 operates variable selection in BO through an MMD-based
304 measure of sensitivity [Spagnol et al., 2019] and is detailed
305 in Appendix C, whereas Dropout [Li et al., 2017] ran-
306 domly selects half of the contextual variable for optimiza-
307 tion. Next, CaBO [Lee et al., 2020] performs vanilla BO
308 over $[\mathbf{x}, \mathbf{z}]$, using a cost-weighted acquisition function. The
309 cost model employed here is a smoothed version of our non-
310 continuous cost model, using a Gaussian curve. Finally, CBO
311 refers to the Contextual BO framework proposed by Krause
312 and Ong [2011]. As a way to assess the impact of contextual
313 variables and selection mechanisms, we also report CUBO
314 and VBO: Context-Unaware BO over the designs \mathbf{x} only and
315 Vanilla BO over both design and contextual variables $[\mathbf{x}, \mathbf{z}]$.

316 **Implementation details.** We fix the hyperparameters of
317 SADCBO to $\eta = 0.8, Q = 10, \gamma_t = 0.8 \forall t$. For the GP
318 surrogate, we use a squared-exponential kernel with in-
319 dependent lengthscales for each variable, learned through
320 marginal likelihood maximization. We use the UCB ac-
321 quisition strategy, as well as Q -UCB for computing \mathcal{D}_t^Q

Table 1: Methods used in experiments.

Name	Description
Without variable selection	Context-Unaware BO over \mathbf{x} only Vanilla BO over $[\mathbf{x}, \mathbf{z}]$
	Cost-Aware BO over $[\mathbf{x}, \mathbf{z}]$ [Lee et al., 2020]
	Contextual BO using all contexts \mathbf{z} [Krause and Ong, 2011]
With variable selection	Randomly drop half of context variables [Li et al., 2017]
	Maximum mean discrepancy-driven BO [Spagnol et al., 2019]
	Sensitivity analysis-driven CBO (This work)

Table 2: Dimensionality of the experiments. For synthetic experiments, additional dimensions stand for (artificial) noise variables, put on top of the design and contextual variables.

Experiment	All dimensions	Design variables	Contextual variables
Portfolio	5	3	2
Yacht	6	4	2
Robot	14	6	8
Molecule	21	3	18
EggHolder	2 + 4	1	1
Hartmann4D	4 + 3	2	2
Hartmann6D	6 + 6	3	3
Ackley	5 + 8	2	3

(Equation (7)) [Wilson et al., 2017]. In all experiments, we assume that any variable, design or contextual ones, has cost $\lambda_j = 1 \forall j \in \{1, \dots, d + c\}$, except in a dedicated study in Section 5.3. Our algorithm is implemented using the BoTorch framework [Balandat et al., 2020]. Code can be accessed at <https://github.com/julienmartinelli/SADCBO>.

5.1 EXPERIMENTS

We benchmark on 4 real-world and 4 synthetic experiments (Table 2) described in brief here and detailed in Appendix E.

Portfolio Optimization 5D. This dataset was first introduced by Cakmak et al. [2020]. The goal is to optimize three design variables, which stand for the hyperparameters of a trading strategy, to maximize return under random environmental conditions. There are two contextual variables, namely: bid–ask spread and the borrowing cost.

Yacht Hydrodynamics 6D. This dataset comes from the UCI Machine Learning Repository [Gerritsma et al., 2013]. The optimization problem is to maximize the residuary resistance per unit weight of displacement of a yacht by controlling its 5-dimensional hull geometry coefficients. Design variables are the first four dimensions of the hull geometry coefficients. The contextual variables are the last hull geometry dimension and the Froude number.

Molecule structure optimization 21D. This computational chemistry example consists of optimizing the bond angles in an alanine molecule to determine the lowest energy conformer, i.e., the structure the molecule will likely take in

nature. These problems are complicated by high dimensionality. We consider the Alanine, a molecule with 21 angular variables: 3 key variables based on prior domain knowledge set as design variables, and 18 other angles treated as contextual variables. Molecular energies are calculated with the AMBER forcefield [Case et al., 2023] at each round of BO.

Robot pushing task 14D. We follow Wang et al. [2017] and consider a control parameter tuning problem for robot pushing. This real-world function returns the distance between a designated goal location and two objects being pushed by two robot hands, whose trajectory is determined by 14 parameters specifying the location, rotation, velocity and moving direction, among others. There are 6 design variables and 8 contextual variables.

Synthetic experiments. We also consider four synthetic test functions, (see Table 2 and Appendix E.2 for details). A min-max transformation is performed on the input data, scaling it to the unit cube: $\mathcal{X} \times \mathcal{Z} = [0, 1]^{d+c}$. Similarly, the output is scaled between $[0, 1]$ and a noise term $\varepsilon \sim \mathcal{N}(0, \sigma_{\text{noise}}^2)$ is added with $\sigma_{\text{noise}}^2 = 0.001$. The contextual variable distribution is $p(\mathbf{z}) = \mathcal{U}([0, 1]^c)$.

5.2 RESULTS

Real-world experiments. In each plot from Figure 2, we report the best value found by each baseline as a function of the number of iterations. In real-world experiments (Figure 2a), SADCBO (in red with white markers) quickly converges to the optimum. SADCBO consistently outperforms the first baselines VBO and CUBO, even though in the Molecular Shape example, SADCBO and CUBO perform on par due to the good choices of the domain experts on the design variables. Except for the Robot Pushing task, the difference between SADCBO and CBO (in blue) is marginal in the real-world experiments. The latter enhances the surrogate model with information from sampled contexts, while our method may even optimize selected contextual variables if needed. Given that these baselines perform similarly, combined with the observation that optimizing only design variables (CUBO, in yellow) produces poor results for the Portfolio and Yacht problems, we can conclude that contextual variables play a significant part in maximizing these two objectives. The cost-aware BO baseline CaBO performs poorly in all tasks. Dropout and MMDBO consistently underperforms, except on the Yacht example for the latter. These baselines perform variable selection in a random manner for Dropout and using Hilbert-Schmidt Independence Criterion for MMDBO [Gretton et al., 2007], two strategies that do not seem to surpass the Feature Collapse method implemented in SADCBO. This observation highlights the need for an informed variable selection strategy. In-depth findings for the Molecule experiment are presented in Appendix E.1 and provide additional explanations as to why SADCBO clearly outperforms MMDBO and Dropout.

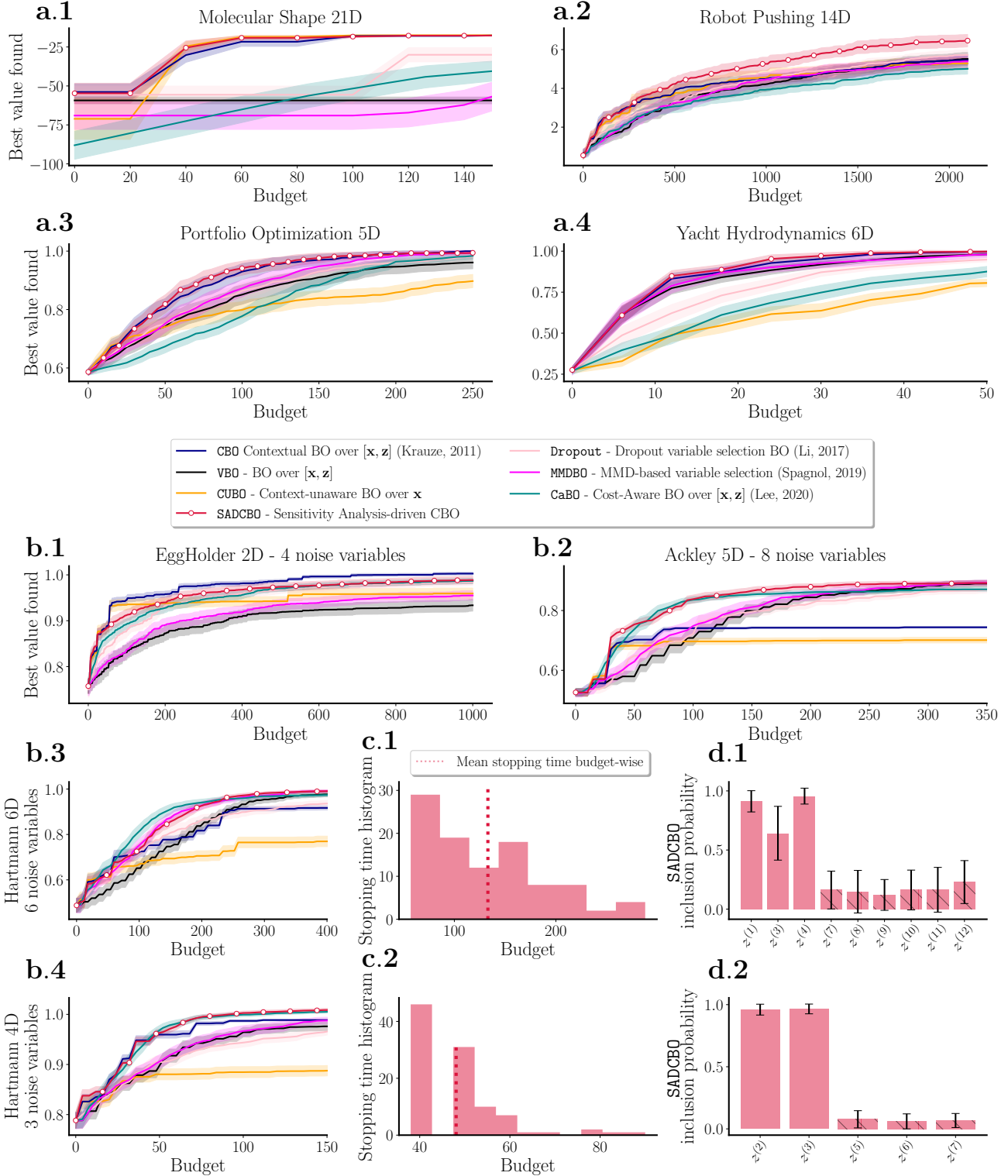


Figure 2: Benchmark of the different methods. **(a)** On real-world datasets, SADCBO (red curve with white markers) performs on par with other baselines and is the top performer for the Robot Pushing task. **(b)** On synthetic functions, SADCBO outperforms other baselines in three cases out of four. **(c)** Histograms of phase switching criteriorng time for SADCBO computed for the Hartmann6D (**c.1**) and Hartmann4D problems (**c.2**). **(d)** Inclusion probability of each contextual variable for SADCBO computed for the Hartmann6D (**d.1**) and Hartmann4D problems (**d.2**). Each panel shows the mean ± 2 standard error across $N = 100$ trials.

399 **Synthetic experiments.** Figure 2b displays the best value
 400 found by each baseline for synthetic functions. SADCBO
 401 ranks first on 3 out of 4 examples, closely followed by the
 402 cost-aware baseline CaBO, which performs much better on
 403 synthetic experiments than on the real-world ones. The con-
 404 textual BO baseline CBO that obtained second to best results
 405 in real-world experiments, is now less performant, due to
 406 the fact that it does not optimize the context, similarly as
 407 CUBO. This seems to be particularly critical for Ackley5D,
 408 whereas for Hartmann6D/Hartmann4D, simply enhancing
 409 the surrogate with contextual variable observation already
 410 leads to a large performance gap between CUBO and CBO.
 411 Lastly, VBO does a poor job as it optimizes every variable,
 412 thus spending a large fraction of the budget every iteration.

413 For Hartmann6D and Hartmann4D, Figure 2c reports the
 414 time at which SADCBO’s switching criterion (Equation (12))
 415 kicks in, in proportion to the total budget, demonstrating
 416 that both phases are leveraged in our approach.

417 Finally, Figure 2d reports the sensitivity indices computed at
 418 each iteration for each contextual variable, averaged across
 419 whole trajectories of multiple trials. For Hartmann6D, the re-
 420 sults match the Sobol sensitivity analysis results (Table S1),
 421 even though global sensitivity indices may differ from sensi-
 422 tivity indices with respect to the function optimum. Similar
 423 findings apply to Hartmann4D (Table S2). Results for other
 424 problems can be found in Figure S2.

Main takeaways. Quantitatively, SADCBO achieves the best overall performances, ranking first in 7 out of 8 problems, although other methods obtained comparable performances on 5 out of 8 problems.

The second-best and third-best methods, CBO and MMDBO, both severely underperform in two examples (Ackley and Hartmann6 for CBO, Molecular Shape and EggHolder for MMDBO). While the improvements provided by SADCBO may seem marginal, they are consistent across the benchmark.

We hypothesize that this consistent behavior stems from our two-stage approach, which allows SADCBO to be versatile. SADCBO can handle both cases where the impact of the contextual variables on the function is limited (hence it is not worth spending budget to control them) and cases where spending budget leads to informative queries are simultaneously well-handled. For instance, SADCBO effectively reverted to a CBO algorithm in the Molecular Shape problem, due to an optimization phase mostly triggered at the end of the run. Meanwhile, for the Ackley function, the optimization phase was triggered in the first quarter of the budget on average, leading to SADCBO outperforming CBO.

5.3 SENSITIVITY ANALYSIS

We now report experiments assessing the robustness of SADCBO’s performance to several modifications, either at the hyperparameter level or at the experiment setting level. The latter includes assessing performance when increasing the number of noise variables, varying the contextual variable query cost, or varying the surrogate model. Next, additional experiments illustrate the sound behavior of the proposed phase switching criterion implemented in SADCBO.

Number of irrelevant contextual variables. We compare the performance reached by SADCBO when adding an increasingly larger number of noise variables and find that even for a large number of irrelevant contextual variables, SADCBO reaches top performance on 3 out of 4 examples (Figure S3). The gap in performance between SADCBO and CaBO, Dropout and MMDBO seems to overall grow with the number of nuisance variables, in favor of SADCBO.

Contextual variables optimization cost. We investigate four different values for the query cost of contextual variables (Figure S4). For extremely cheap contextual variables $\lambda_j = 0.1$ for all j , that is, ten times cheaper than a design variable, VBO performs favorably, as optimizing over all inputs $[x, z]$ is cheap. SADCBO remains competitive in this configuration, even though MMDBO and CaBO perform on par. For a moderate cost $\lambda_j = 1$ (the cost model considered in Figure 2), SADCBO obtains the lowest average rank over all four test functions. For expensive contextual variables, $\lambda_j = 3$ or $\lambda_j = 10$, CaBO seems overall more suitable, although closely followed by SADCBO, and CBO.

Sparsity-enforcing surrogates with SADCBO. As SADCBO relies on a posterior sensitivity analysis to select the relevant contextual variables, and is hence agnostic to the choice of GP surrogate model, it can be combined with other methods that induce sparsity via the GP surrogate. One such method is by Eriksson and Jankowiak [2021], who introduced a sparsity-enforcing GP surrogate equipped with a horseshoe prior on the square inverse lengthscales, coined SAASBO. In Figure 3, we compare SADCBO with the combined method SAASBO+SADCBO, with both having the same hyperparameters. We observe that SAASBO+SADCBO improves over just SAASBO in all the synthetic examples, and is also better than SADCBO in two out of four examples. Note that the performance of SAASBO+SADCBO may further improve through hyperparameter tuning.

SADCBO phase switching criterion. We ensure that the criterion is well-behaved: the more information about the output is contained in the contextual variables, the later the phase switching occurs (Figure S5). Even though the stopping criterion was initially devised for vanilla BO, its application in a CBO setting is fruitful. Figure 4 further illustrates the soundness of the phase switching criterion.

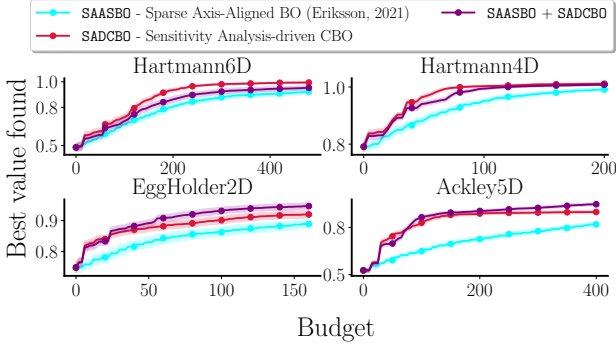


Figure 3: Combining SADCBO with sparsity-enforcing surrogate SAASBO. For any variable, the associated query cost is 1. $p(\mathbf{z}) = \mathcal{U}([0, 1]^c)$. The combination is fruitful and improves the performances of SAASBO.

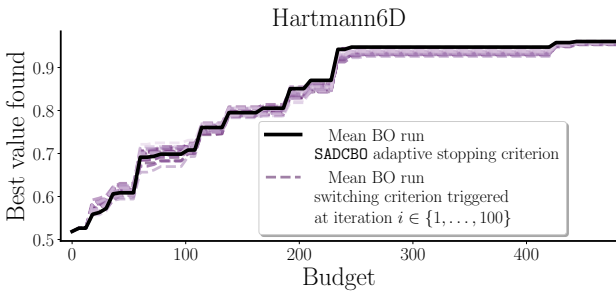


Figure 4: Assessing SADCBO’s phase switching criterion on the Hartmann6D function. The iteration selected by the adaptive stopping criterion implemented in SADCBO yields one of the best BO trials. Each curve is computed as an average of 10 different random seeds.

duced SADCBO, an algorithm designed to select relevant context variables affecting the experimental outcomes by efficiently leveraging information present in both the observational and the interventional data. SADCBO results in more adequate surrogate models, and ensures the reproducibility of experiments by controlling for such relevant variables. In that respect, SADCBO should be used for practical applications where contextual variables can have an influence while being controllable. This includes, e.g., the development of new high-throughput materials or drugs, where machine learning strategies are being increasingly used [Zhang et al., 2020, Gómez-Bombarelli et al., 2018]. SADCBO can also be combined with any GP surrogate. Thus, if a practitioner believes that a specific contextual variable should be included, this can be easily achieved. Conversely, the variable selection procedure could be generalized to discard design variables as well. Lastly, recent work [Branchini et al., 2023] proposed to perform BO under the assumption that the input variables and the output are linked by a causal directed acyclic graph, learning the graph whilst maximizing the objective function. Despite its high computational complexity, applying this technique to our particular problem might be promising.

Limitations and future work. To achieve cost efficiency, SADCBO integrates the query cost at the variable selection level and employs an early stopping criterion. The latter only depends on an upper bound on the instantaneous regret difference and is therefore not cost-aware. Adding a notion of remaining budget to this criterion would certainly benefit our approach. On a similar note, while our algorithm incorporates cost, more effort could be put into specifying the costs. In our experiments, they were set to 1 for all variables to prevent bias in the results, and we carried out an ablation study with different costs in Section 5.3. Yet, it is worth mentioning that our method is compatible with the inference of black-box, input-dependent costs, similarly to CaBO [Lee et al., 2020]. One would simply need to modify Equation (9), replacing λ_j by the learned cost. An interesting avenue for future work would be to elicit knowledge of experimental costs from domain experts in real-world situations.

Acknowledgements

JM acknowledges the support of the Research Council of Finland under the HEALED project (grant 13342077). AB, AT, STJ, and PR were supported by the Research Council of Finland Flagship programme: Finnish Center for Artificial Intelligence FCAI. AT further acknowledges funding from the European Union’s Horizon 2020 research and innovation programme under the Marie Skłodowska-Curie grant agreement No. 101059891. SJS and SK were supported by the UKRI Turing AI World-Leading Researcher Fellowship, [EP/W002973/1].

6 CONCLUSION

In this paper, we extended Contextual BO [Krause and Ong, 2011] to settings in which the contextual variables may be not only observed but also optimized at a cost. We intro-

544 **References**

- 545 Milad Abolhasani and Keith A. Brown. Role of AI in experimental materials science. *MRS Bulletin*, 2023.
- 546
- 547 Vahan Arsenyan, Antoine Grosnit, and Haitham Bou-
548 Ammar. Contextual causal Bayesian optimisation. *arXiv
549 preprint arXiv:2301.12412*, 2023.
- 550 Maximilian Balandat, Brian Karrer, Daniel Jiang, Samuel
551 Daulton, Ben Letham, Andrew G Wilson, and Eytan Bak-
552 shy. BoTorch: A Framework for Efficient Monte-Carlo
553 Bayesian Optimization. In *Advances in Neural Information
554 Processing Systems (NeurIPS)*, 2020.
- 555 Ilija Bogunovic, Jonathan Scarlett, Stefanie Jegelka, and
556 Volkan Cevher. Adversarially robust optimization with
557 Gaussian processes. In *Advances in Neural Information
558 Processing Systems (NeurIPS)*, 2018.
- 559 Nicola Branchini, Virginia Aglietti, Neil Dhir, and
560 Theodoros Damoulas. Causal entropy optimization. In
561 *Proceedings of the International Conference on Artificial
562 Intelligence and Statistics (AISTATS)*, 2023.
- 563 Sait Cakmak, Raul Astudillo Marban, Peter Frazier, and
564 Enlu Zhou. Bayesian Optimization of Risk Measures.
565 In *Advances in Neural Information Processing Systems
566 (NeurIPS)*, pages 20130–20141, 2020.
- 567 David Case, H. Metin Aktulga, Kellon Belfon, Ido Ben-
568 Shalom, Joshua Berryman, Scott Brozell, David Cerutti,
569 Thomas Cheatham, Gerardo Andrés Cisneros, Vinícius
570 Cruzeiro, Tom Darden, Negin Forouzesh, George Gi-
571 ambasu, Timothy Giese, Michael Gilson, Holger Gohlke,
572 Andreas Götz, Julie Harris, Saeed Izadi, and Peter Koll-
573 man. Amber 2023, 2023.
- 574 David Eriksson and Martin Jankowiak. High-dimensional
575 Bayesian optimization with sparse axis-aligned subspaces.
576 In *Proceedings of the Thirty-Seventh Conference on Un-
577 certainty in Artificial Intelligence (UAI)*, 2021.
- 578 Lincan Fang, Esko Makkonen, Milica Todorović, Patrick
579 Rinke, and Xi Chen. Efficient Amino Acid Conformer
580 Search with Bayesian Optimization. *Journal of Chemical
581 Theory and Computation*, 17, 2021.
- 582 Roman Garnett. *Bayesian Optimization*. Cambridge Uni-
583 versity Press, 2023.
- 584 J. Gerritsma, R. Onnink, and A. Versluis. Yacht Hydrody-
585 namics. UCI Machine Learning Repository, 2013.
- 586 Rafael Gómez-Bombarelli, Jennifer N. Wei, David Duve-
587 naud, José Miguel Hernández-Lobato, Benjamín Sánchez-
588 Lengeling, Dennis Sheberla, Jorge Aguilera-Iparraguirre,
589 Timothy D. Hirzel, Ryan P. Adams, and Alán Aspuru-
590 Guzik. Automatic Chemical Design Using a Data-Driven
591 Continuous Representation of Molecules. *ACS Central
592 Science*, 4(2):268–276, 2018.
- 593 Arthur Gretton, Kenji Fukumizu, Choon Teo, Le Song, Bern-
594 hard Schölkopf, and Alex Smola. A kernel statistical test
595 of independence. In *Advances in Neural Information
596 Processing Systems*, 2007.
- 597 Arthur Gretton, Karsten M Borgwardt, Malte J Rasch, Bern-
598 hard Schölkopf, and Alexander Smola. A kernel two-
599 sample test. *Journal of Machine Learning Research*, 13:
600 723–773, 2012.
- 601 Kate Higgins, Maxim Ziatdinov, Sergei Kalinin, and
602 Mahshid Ahmadi. High-throughput study of antisol-
603 vents on the stability of multicomponent metal halide per-
604 ovskites through robotics-based synthesis and machine
605 learning approaches. *Journal of the American Chemical
606 Society*, 143(47), 2021.
- 607 Hisham Husain, Vu Nguyen, and Anton van den Hengel.
608 Distributionally robust Bayesian optimization with φ -
609 divergences. In *Advances in Neural Information Process-
610 ing Systems (NeurIPS)*, 2023.
- 611 Hideaki Ishibashi, Masayuki Karasuyama, Ichiro Takeuchi,
612 and Hideitsu Hino. A stopping criterion for Bayesian
613 optimization by the gap of expected minimum simple
614 regrets. In *Proceedings of The International Conference
615 on Artificial Intelligence and Statistics (AISTATS)*, 2023.
- 616 Johannes Kirschner, Ilija Bogunovic, Stefanie Jegelka, and
617 Andreas Krause. Distributionally Robust Bayesian Opti-
618 mization. In *Proceedings of the International Conference
619 on Artificial Intelligence and Statistics (AISTATS)*, 2020.
- 620 Ksenia Korovina, Sailun Xu, Kirthevasan Kandasamy,
621 Willie Neiswanger, Barnabas Poczos, Jeff Schneider, and
622 Eric Xing. ChemBO: Bayesian Optimization of Small Or-
623 ganic Molecules with Synthesizable Recommendations.
624 In *International Conference on Artificial Intelligence and
625 Statistics (AISTATS)*, 2020.
- 626 Andreas Krause and Cheng Ong. Contextual Gaussian Pro-
627 cess Bandit Optimization. In *Advances in Neural Infor-
628 mation Processing Systems (NeurIPS)*, 2011.
- 629 Eric Hans Lee, Valerio Perrone, Cedric Archambeau, and
630 Matthias Seeger. Cost-aware Bayesian Optimization.
631 *arXiv preprint arXiv:2003.10870*, 2020.
- 632 Eric Hans Lee, David Eriksson, Valerio Perrone, and
633 Matthias Seeger. A Nonmyopic Approach to Cost-
634 Constrained Bayesian Optimization. In *Proceedings of
635 the Thirty-Seventh Conference on Uncertainty in Artifi-
636 cial Intelligence (UAI)*, 2021.
- 637 Cheng Li, Sunil Gupta, Santu Rana, Vu Nguyen, Svetha
638 Venkatesh, and Alistair Shilton. High dimensional
639 Bayesian optimization using dropout. In *Proceedings
640 of the International Joint Conference on Artificial Intelli-
641 gence (IJCAI)*, 2017.

- 642 Sulin Liu, Qing Feng, David Eriksson, Benjamin Letham,
 643 and Eytan Bakshy. Sparse Bayesian Optimization. In
 644 *Proceedings of the International Conference on Artificial*
 645 *Intelligence and Statistics (AISTATS)*, 2023.
- 646 Anastasia Makarova, Huibin Shen, Valerio Perrone, Aaron
 647 Klein, Jean Baptiste Faddoul, Andreas Krause, Matthias
 648 Seeger, and Cedric Archambeau. Automatic termination
 649 for hyperparameter optimization. In *Proceedings of the*
 650 *First International Conference on Automated Machine*
 651 *Learning*, 2022.
- 652 Philip W. Nega, Zhi Li, Victor Ghosh, Janak Thapa, Shi-
 653 jing Sun, Noor Titan Putri Hartono, Mansoor Ani Na-
 654 jeeb Nellikkal, Alexander J. Norquist, Tonio Buonassisi,
 655 Emory M. Chan, and Joshua Schrier. Using automated
 656 serendipity to discover how trace water promotes and
 657 inhibits lead halide perovskite crystal formation. *Applied*
 658 *Physics Letters*, 119(4), 2021.
- 659 C. Rasmussen and C. Williams. *Gaussian Processes for*
 660 *Machine Learning*. MIT Press, 2006.
- 661 Paul Rolland, Jonathan Scarlett, Ilija Bogunovic, and Volkan
 662 Cevher. High-Dimensional Bayesian Optimization via
 663 Additive Models with Overlapping Groups. In *Proceed-*
 664 *ings of the International Conference on Artificial Intel-*
 665 *ligence and Statistics (AISTATS)*, 2018.
- 666 Artun Saday, Yaşar Cahit Yıldırım, and Cem Tekin. Robust
 667 Bayesian satisficing. In *Advances in Neural Information*
 668 *Processing Systems (NeurIPS)*, 2023.
- 669 Romelia Salomon Ferrer, David Case, and Ross Walker. An
 670 overview of the Amber biomolecular simulation package.
 671 *Wiley Interdisciplinary Reviews: Computational Mole-*
 672 *cular Science*, 3, 2013.
- 673 Isaac Sebenius, Topi Paananen, and Aki Vehtari. Feature
 674 Collapsing for Gaussian Process Variable Ranking. In
 675 *Proceedings of The International Conference on Artificial*
 676 *Intelligence and Statistics (AISTATS)*, 2022.
- 677 Yihang Shen and Carl Kingsford. Computationally Efficient
 678 High-Dimensional Bayesian Optimization via Variable
 679 Selection. *arXiv preprint arXiv:2109.09264*, 2021.
- 680 I.M Sobol. Global sensitivity indices for nonlinear mathe-
 681 matical models and their Monte Carlo estimates. *Math-*
 682 *ematics and Computers in Simulation*, 55(1):271–280,
 683 2001.
- 684 Adrien Spagnol, Rodolphe Le Riche, and Sébastien Da
 685 Veiga. Bayesian optimization in effective dimensions
 686 via kernel-based sensitivity indices. In *Proceedings of*
 687 *the International Conference on Applications of Statistics*
 688 *and Probability in Civil Engineering (ICASP)*, 2019.
- Niranjan Srinivas, Andreas Krause, Sham M. Kakade,
 689 and Matthias W. Seeger. Information-Theoretic Regret
 690 Bounds for Gaussian Process Optimization in the Bandit
 691 Setting. *IEEE Transactions on Information Theory*, 58
 692 (5):3250–3265, 2012.
- 693
- 694 Sebastian Shenghong Tay, Chuan Sheng Foo, Daisuke
 695 Urano, Richalynn Chiu Xian Leong, and Bryan
 696 Kian Hsiang Low. Bayesian optimization with cost-
 697 varying variable subsets. In *Advances in Neural Infor-*
 698 *mation Processing Systems (NeurIPS)*, 2023.
- 699 Saul Toscano-Palmerin and Peter I. Frazier. Bayesian op-
 700 timization with expensive integrands. *SIAM Journal on*
 701 *Optimization*, 32(2):417–444, 2022.
- 702 Theja Tulabandhula and Cynthia Rudin. Robust optimiza-
 703 tion using machine learning for uncertainty sets. *arXiv*
 704 *preprint arXiv:1407.1097*, 2014.
- 705 Zi Wang, Chengtao Li, Stefanie Jegelka, and Pushmeet
 706 Kohli. Batched high-dimensional Bayesian optimization
 707 via structural kernel learning. In *Proceedings of the 34th*
 708 *International Conference on Machine Learning (ICML)*,
 709 2017.
- 710 James T. Wilson, Riccardo Moriconi, Frank Hutter, and
 711 Marc Peter Deisenroth. The reparameterization trick for
 712 acquisition functions. *arXiv preprint arXiv:1712.00424*,
 713 2017.
- 714 Yichi Zhang, Daniel W Apley, and Wei Chen. Bayesian
 715 optimization for materials design with mixed quantitative
 716 and qualitative variables. *Scientific Reports*, 10(1):1–13,
 717 2020.
- 718 Juliusz Ziomek and Haitham Bou-Ammar. Are Random De-
 719 compositions all we need in High Dimensional Bayesian
 720 Optimisation? In *Proceedings of the International Con-*
 721 *ference on Machine Learning (ICML)*, 2023.

Learning Relevant Contextual Variables Within Bayesian Optimization (Supplementary Material)

¹Inserm Bordeaux Population Health, Vaccine Research Institute, Université de Bordeaux, Inria Bordeaux Sud-ouest, France

²Department of Computer Science, Aalto University, Helsinki, Finland

³Department of Applied Physics, Aalto University, Helsinki, Finland

⁴Univ. Lille, CNRS, Centrale Lille, UMR 9189 CRISTAL, F-59000 Lille, France

⁵Department of Computer Science, University of Manchester, Manchester, United Kingdom

APPENDIX

Outline. The Appendix is organized as follows. In Appendix A, we provide a flowchart summarizing the proposed method SADCBO. In Appendix B, we provide further details about the phase switching criterion introduced in Section 3.2. In Appendix C, we provide more details about one of the baselines used in the main text, based on maximum mean discrepancy. Appendix D contains further experimental results regarding:

- Phase switching time and sensitivity-based inclusion probabilities of contextual variables found by SADCBO for additional test functions (Figure S2).
 - Varying the number of irrelevant contextual variables (Figure S3).
 - Varying contextual variables query cost (Figure S4).
 - The distribution of phase switching times for SADCBO (Figure S5).
 - Varying SADCBO hyperparameters (Appendix D.1 and Figure S6).

Finally, Appendix E contains a description of the real-world experiments performed throughout the paper, along with the analytical expressions of the synthetic examples used.

A FLOWCHART OF THE ALGORITHM

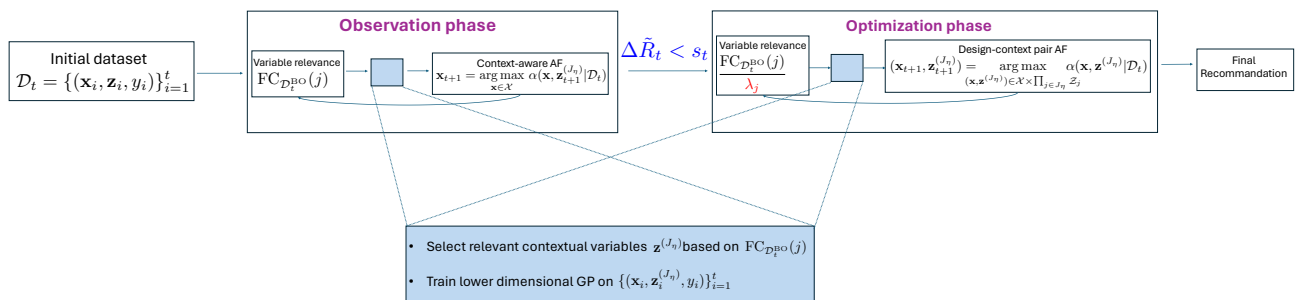


Figure S1: Flowchart of the proposed method SADCBO.

*Work done while at Aalto University.

B PHASE SWITCHING CRITERION

The phase switching criterion we employ is derived from the stopping criterion from Ishibashi et al. [2023]. The absolute difference of expected minimum simple regrets $\Delta R_t := |R_t - R_{t-1}|$ can be upper bounded with probability $1 - \delta$ by $\Delta \tilde{R}_t$, a quantity defined in Equation (11). Directly quoting the work of Ishibashi et al. [2023], the rationale behind this criterion reads as follows: “By evaluating the difference between the expected minimum simple regrets, we can stop BO without knowing f^* , because it indicates that the search efficiency is low and there is almost no improvement in the objective value. However, it is generally difficult to calculate ΔR_t analytically”. Next, any stopping criterion involves the computation of some sort of threshold. Ishibashi et al. [2023] exploit the fact that their upper bound $\Delta \tilde{R}_t$ can itself be upper bounded by a quantity (introduced in [Ishibashi et al., 2023, Equation 10]), whose convergence speed to zero is limited by a specific term, s_t (Equation 12). s_t can be computed analytically and therefore yields an adaptive threshold.

Finally, Equation (11) involves a sequence $\kappa_{\delta,t-1}$:

$$\kappa_{\delta,t-1} = \max_{\mathbf{v} \in \mathcal{D}_{t-1}} \text{UCB}_\delta(\mathbf{v}) - \max_{\mathbf{v} \in \mathcal{V}} \text{LCB}_\delta(\mathbf{v}), \quad (\text{S1})$$

where $\text{UCB}_\delta(\mathbf{v}) = \mu_t(\mathbf{v}|\mathcal{D}_t) + \beta_t^{1/2} \sigma_t(\mathbf{v}|\mathcal{D}_t)$ and $\text{LCB}_\delta(\mathbf{v}) = \mu_t(\mathbf{v}|\mathcal{D}_t) - \beta_t^{1/2} \sigma_t(\mathbf{v}|\mathcal{D}_t)$. $\beta_t^{1/2}$ is a trade-off parameter between exploration and exploitation that depends on δ [Srinivas et al., 2012]. $\kappa_{\delta,t-1}$ is a quantity that was first introduced by Makarova et al. [2022, Section 3.2] as an upper bound for the simple regret of the surrogate, which directly flows from the bounds provided by Srinivas et al. [2012] for well-calibrated surrogates.

Heuristically, one can think of our setting as applying the stopping criterion to $\mathbf{x} \mapsto f(\mathbf{x}, \mathbf{z})$, a stochastic black-box function with $\mathbf{z} \sim p(\mathbf{z})$. Upon satisfaction of this criterion, we switch to the optimization of $(\mathbf{x}, \mathbf{z}) \mapsto f(\mathbf{x}, \mathbf{z})$ where some contextual variables are optimized, and some others are still sampled from $p(z^{(j)})$.

C MAXIMUM MEAN DISCREPANCY-BASED VARIABLE SELECTION

Spagnol et al. [2019] introduced a BO algorithm with a variable selection procedure based on the Hilbert Schmidt Independence Criterion (HSIC). This measure can be used in our setting as well. We now briefly describe how it is defined.

As introduced in the main text, let $\mathcal{Z} \subset \mathbb{R}^c$ be the space of contextual variables, and \mathcal{H} be a Hilbert space of \mathbb{R} -valued functions on \mathcal{Z} . Assume that $k : \mathcal{Z} \times \mathcal{Z} \rightarrow \mathbb{R}$ is the unique positive definite kernel associated with the Reproducing Kernel Hilbert Space \mathcal{H} . Let $\mu_{\mathbb{P}_Z}$ be the kernel mean embedding of the distribution \mathbb{P}_Z , $\mu_{\mathbb{P}_Z} := \mathbb{E}_Z[k(Z, \cdot)] = \int_{\mathcal{Z}} k(\mathbf{z}, \cdot) d\mathbb{P}_Z$. Kernel embeddings of probability measures provide a distance between distributions between their embeddings in the Hilbert Space \mathcal{H} , named Maximum Mean Discrepancy (MMD, [Gretton et al., 2012]):

$$\text{MMD}(\mathbb{P}_Z, \mathbb{P}_Y) = \|\mu_{\mathbb{P}_Z} - \mu_{\mathbb{P}_Y}\|_{\mathcal{H}}^2. \quad (\text{S2})$$

For two random variables $Z \sim \mathbb{P}_Z$ on \mathcal{H} and $Y \sim \mathbb{P}_Y$ on \mathcal{G} , the HSIC is the squared MMD between the product distribution \mathbb{P}_{ZY} and the product of its marginals $\mathbb{P}_Z \mathbb{P}_Y$,

$$\text{HSIC}(Z, Y) = \text{MMD}^2(\mathbb{P}_{ZY}, \mathbb{P}_Z \mathbb{P}_Y) \quad (\text{S3})$$

$$= \|\mu_{\mathbb{P}_{ZY}} - \mu_{\mathbb{P}_Z \mathbb{P}_Y}\|_{\mathcal{H} \otimes \mathcal{G}}^2 \quad (\text{S4})$$

$$\begin{aligned} &= \mathbb{E}_{Z,Y} \mathbb{E}_{Z',Y'} [k(Z, Z') l(Y, Y')] \\ &\quad + \mathbb{E}_Z \mathbb{E}_Y \mathbb{E}_{Z'} \mathbb{E}_{Y'} [k(Z, Z') l(Y, Y')] \\ &\quad - 2 \mathbb{E}_{Z,Y} \mathbb{E}_{Z'} \mathbb{E}_{Y'} [k(Z, Z') l(Y, Y')]. \end{aligned} \quad (\text{S5})$$

To determine the relevance of a variable $Z^{(i)}$, Spagnol et al. [2019] introduce

$$S^{\text{HSIC}}(Z^{(i)}) = \text{HSIC}(Z^{(i)}, \mathbb{I}(Z \in \mathcal{L}_\gamma)), \quad (\text{S6})$$

with \mathcal{L}_γ a region of interest: the locations where the objective function value is above a threshold γ . This measure reflects how important $Z^{(i)}$ is to reach \mathcal{L}_γ .

We implemented this measure, substituting expectations for empirical means over the dataset \mathcal{D} . We use $\gamma = 0.8$, a threshold identical to the one used for SADCBO in Equation (6). The kernel k is chosen to be a RBF kernel, and l is a linear kernel $l(y, y') = yy'$, a common choice for binary data.

D ADDITIONAL EXPERIMENTAL RESULTS

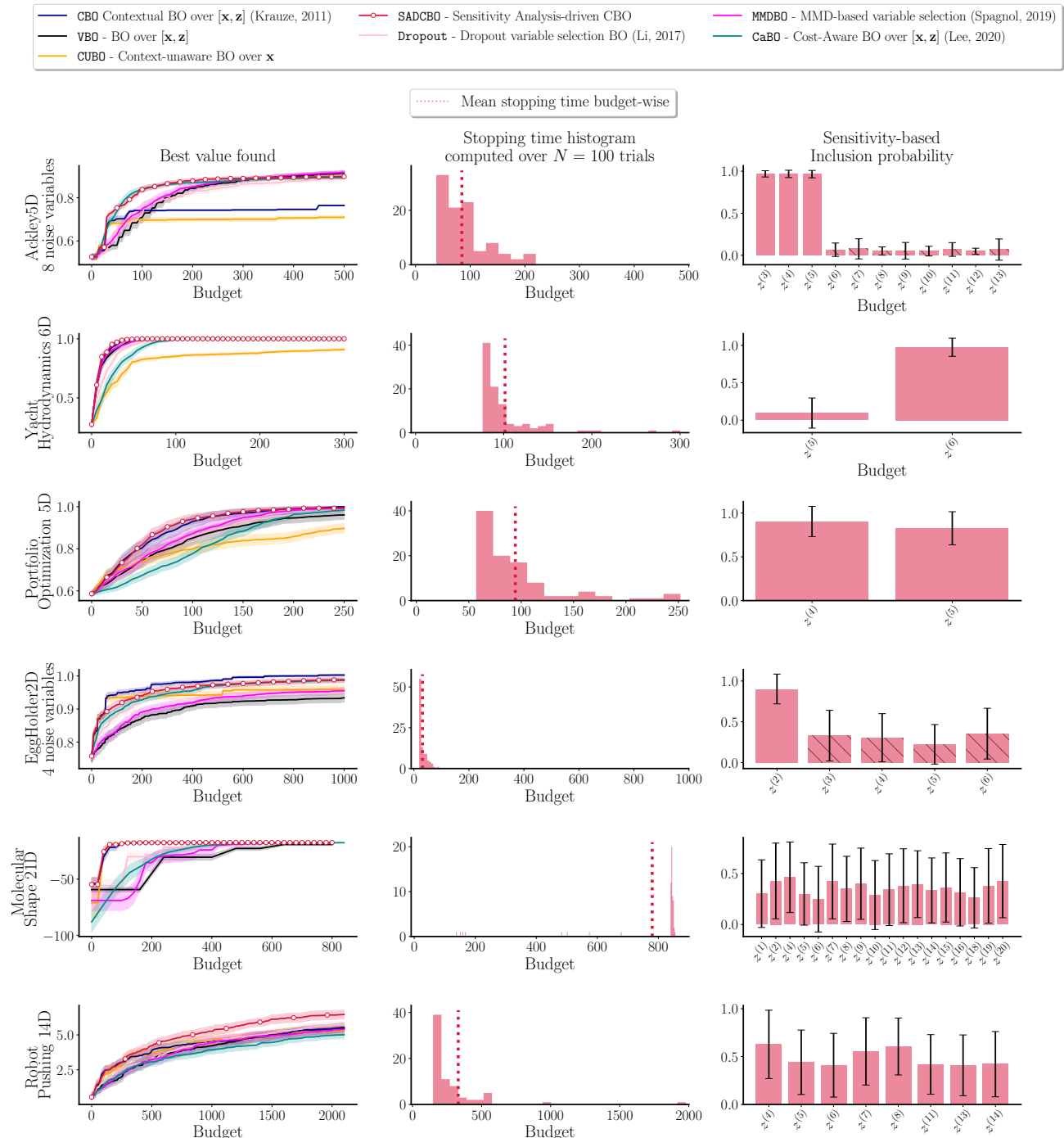


Figure S2: Each row deals with a specific problem. The left panel shows the BO trial results for each baseline. The middle and right panel show statistics related to SADCBO: 1) the phase switching time after which phase II begins and 2) the inclusion probabilities for each contextual variable. Statistics are computed across $N = 100$ BO trials with different seeds.

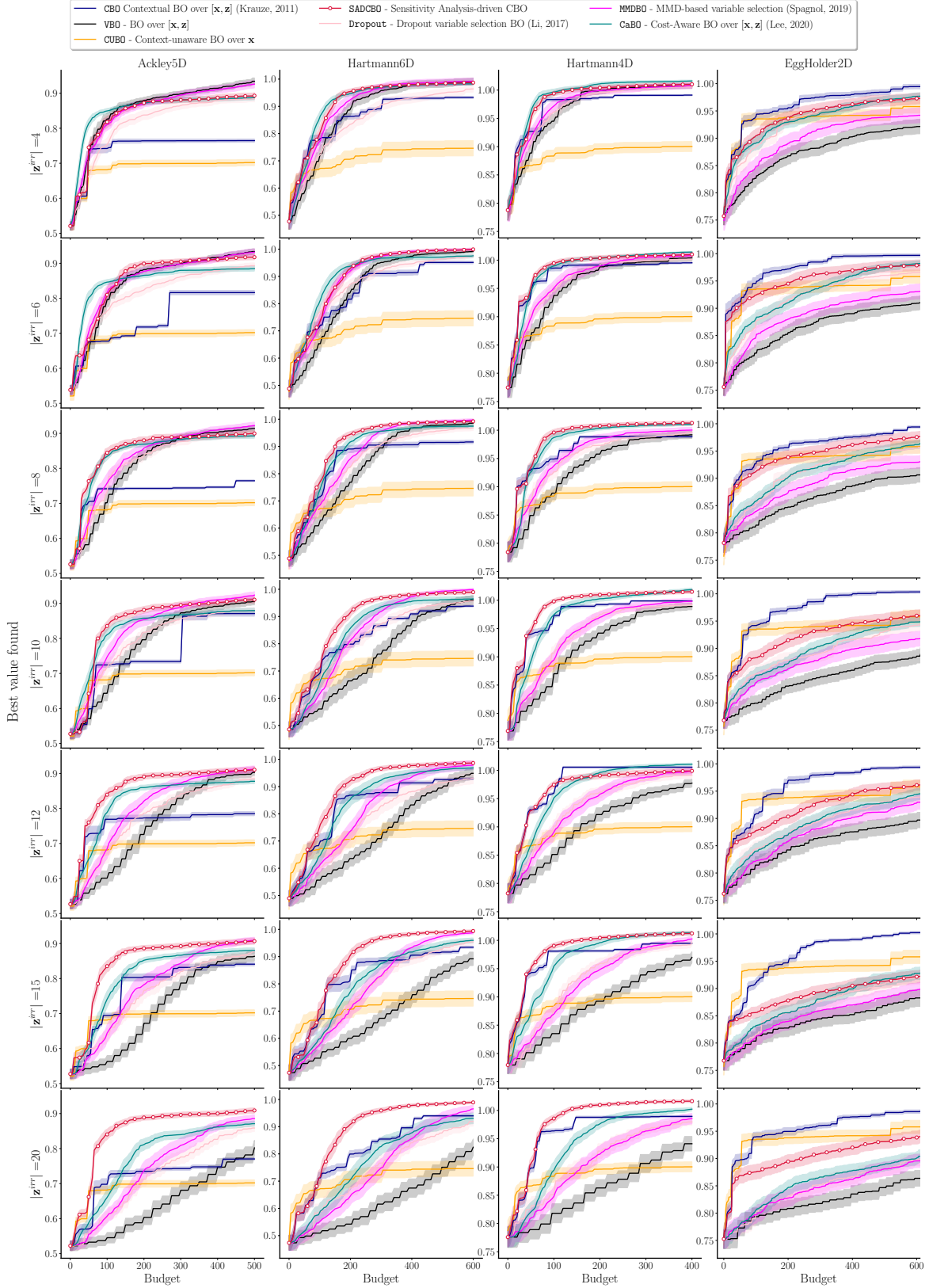


Figure S3: Varying the number of irrelevant contextual variables. For any variable, the associated query cost is 1. $p(\mathbf{z}) = \mathcal{U}([0, 1]^c)$. On the three test functions Ackley5D, Hartmann6D and Hartmann4D, our approach outperforms other baselines even in high dimensions.

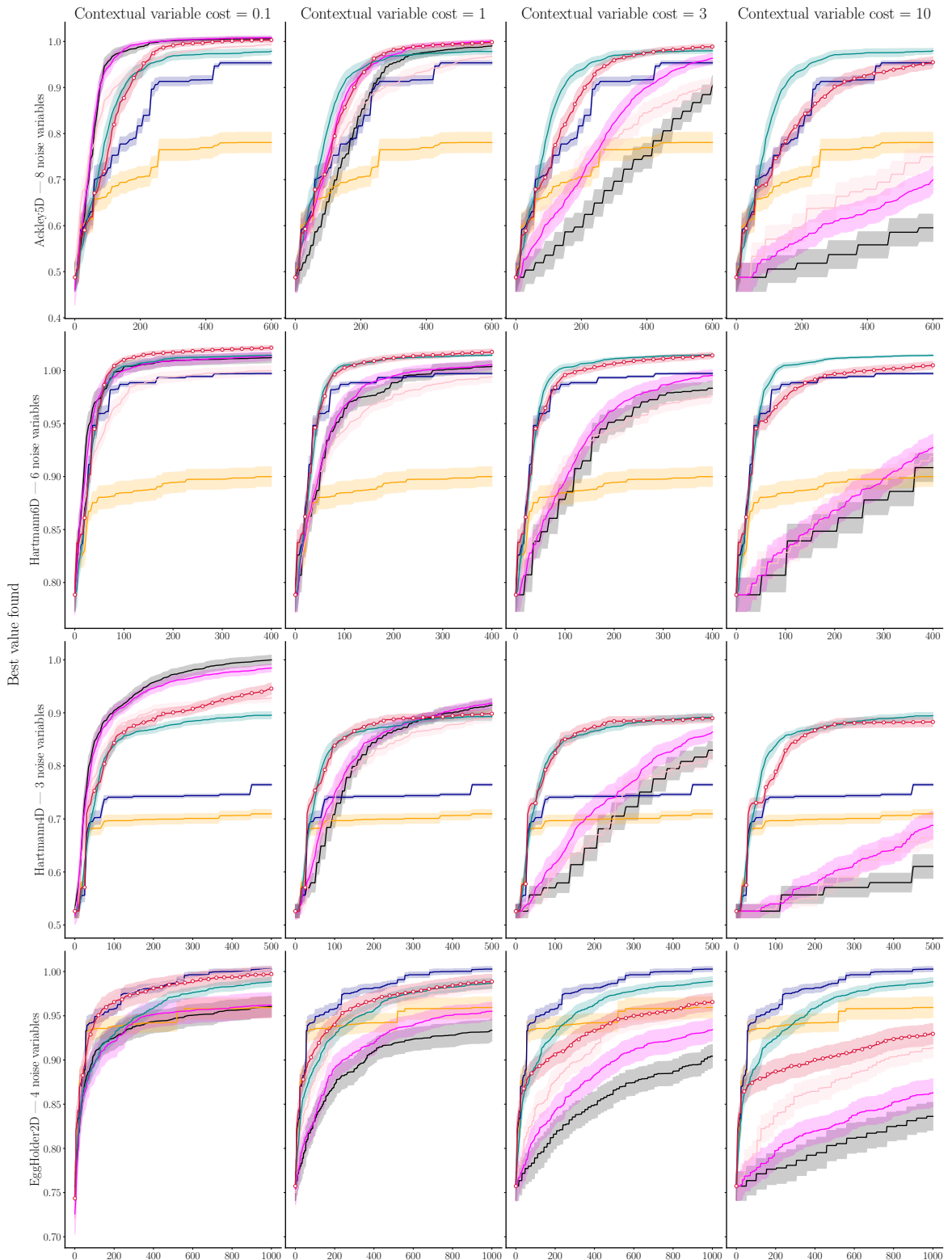
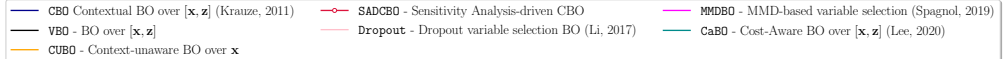


Figure S4: Ablation study on contextual variable query cost. Design variables have cost 1. $p(z) = \mathcal{U}([0, 1]^c)$.

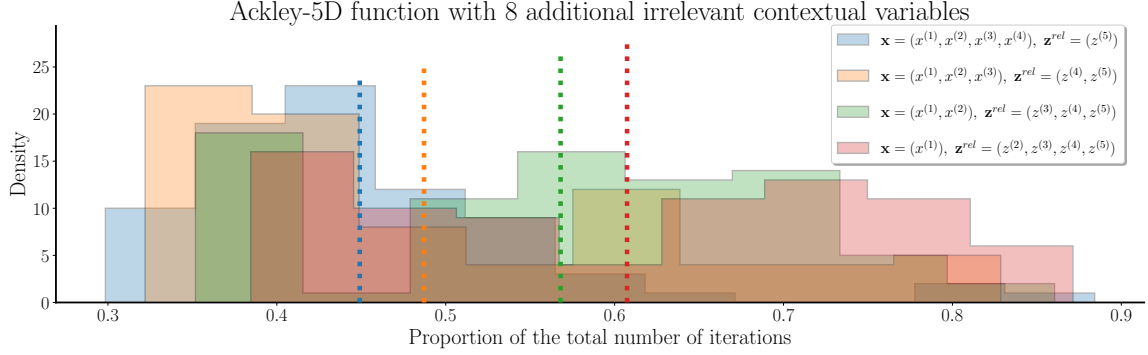


Figure S5: Distribution of phase switching criterion triggering times for SADCBO across $N = 100$ different BO trials. We consider the Ackley5D function with an increasingly larger ratio of relevant contextual variables over design variables, and 8 irrelevant contextual variables. $p(\mathbf{z}) = \mathcal{U}([0, 1]^c)$. For any variable, the associated query cost is 1. As the impact of contextual variables on the output function grows, the number of iterations spent in the observational phase grows as well.

D.1 ADDITIONAL DETAILS ON HYPERPARAMETER VARIATIONS.

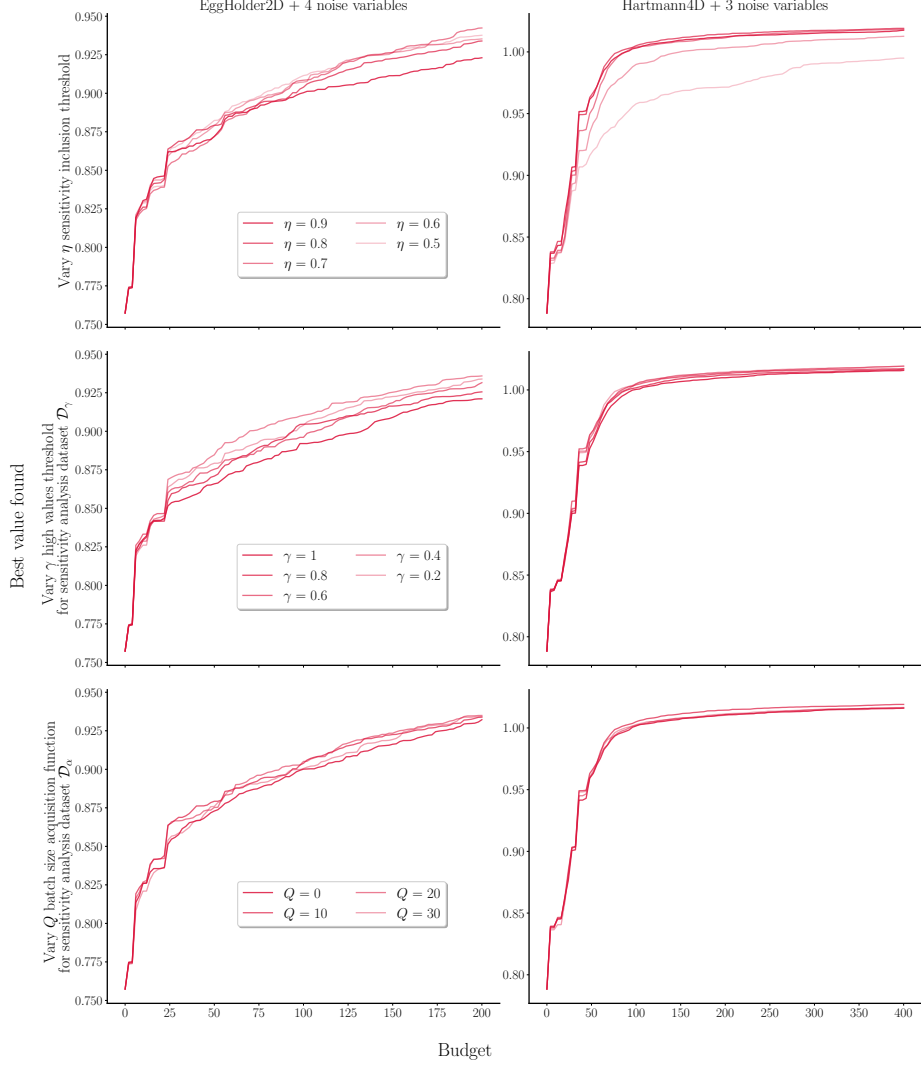


Figure S6: Varying hyperparameters for SADCBO. For any variable, the associated query cost is 1. $p(\mathbf{z}) = \mathcal{U}([0, 1]^c)$. Top: varying η , the contextual variable inclusion threshold over the cumulative sum of sensitivity indices. Middle: varying γ , the threshold used in the creation of the truncated dataset \mathcal{D}^γ from Equation (6). Bottom: varying Q , the size of the dataset \mathcal{D}^Q from Equation (7). η is the most sensitive hyperparameter here.

We vary the 3 hyperparameters of SADCBO: $\eta \in [0, 1]$ the threshold based over the cumulative sum of sensitivity indices, which in turn regulates how many variables are selected every iteration; $\gamma \in [0, 1]$, a threshold upon which a value is considered high enough to have its input added to dataset \mathcal{D}^γ (Equation (6)), used for sensitivity analysis; and Q the size of the dataset \mathcal{D}^Q (Equation (7)).

Figure S6 reports the performances. Unsurprisingly, η stands out as the most stringent parameter: as its value decreases, fewer variables are included, at which point not all relevant ones are selected, leading to reduced performances. Note that in a setting where there are no relevant contextual variables, lower values of η will actually lead to better performances. Then, varying $\gamma \in [0, 1]$ slightly affects the results: γ increasing means that more samples are collected for sensitivity analysis, but these are less relevant for producing a reliable set of variables accounting for the fluctuations at the optimum. Finally, for the examples considered, Q has only a limited effect, close to that of varying γ . This might stem from the fact that batched acquisition functions are notoriously difficult to optimize and may sometimes struggle to enforce diversity.

E EXPERIMENT DETAILS

E.1 REAL-WORLD DATASETS

Portfolio optimization dataset. This dataset was first introduced in [Cakmak et al., 2020]. The goal is to tune the hyper-parameters of a trading strategy so as to maximize return under risk-aversion to random environmental conditions. A software is used to simulate and optimize the evolution of a portfolio over a period of four years using open-source market data. Each evaluation of this simulator returns the average daily return over this period of time under the given combination of hyper-parameters and environmental conditions. Since the simulator is expensive to evaluate, we do not use it directly but perform pool-based Bayesian Optimization using a pool of 3000 points generated according to a Sobol sampling design.

The hyper-parameters to be optimized are the risk and trade aversion parameters and the holding cost multiplier. These variables constitute the design variables. The contextual variables are the bid-ask spread and the borrowing cost.

Yacht hydrodynamics dataset. This dataset comes from the UCI Machine Learning Repository [Gerritsma et al., 2013]. The optimization problem is to maximize the residuary resistance per unit weight of displacement of a yacht by controlling its 5-dimensional hull geometry coefficients. Another optimization variable is the 1-dimensional Froude number. We chose as design variables the first four dimensions of the hull geometry coefficients. The contextual variables are the last hull geometry dimension and the Froude number. Like the Portfolio optimization dataset, we have access to a limited number of samples (≈ 300) and thus perform pool-based Bayesian optimization.

Molecular structure optimization. This case is a computational chemistry challenge. Molecules can adopt different structures that preserve the topology (bonds and bonding types), but have different internal angles. Finding such conformers is a global optimization problem. Here, we are searching for the conformers of alanine — a molecule with structure $C_3H_7NO_2$ — whose energy is calculated at each round of BO with the AMBER force field [Salomon Ferrer et al., 2013, Case et al., 2023]. Alanine provides 33 structural variables to optimize: ten dihedral angles, eleven bond angles, and twelve bond lengths. Conformer search in the full 33-dimensional space is very challenging, but progress has been made with Bayesian optimization recently by reducing the problem to the four most important dihedral angles [Fang et al., 2021]. For the example in this work, three of these four dihedral angles were chosen as the design variables (indices 3, 17, and 21 in the dataset; which denotes dihedral angles d4, d11, and d13 in AMBER notation; d4 is the bond leading to the amino group, d13 the one leading to the hydroxyl group, and d11 is the bond between these two), the rest of the dihedral and bond angles (18 angles) are chosen as the contextual variables, and the bond lengths are kept fixed to facilitate faster simulations. The search space is selected by utilizing molecule domain knowledge in a conservative manner that allows 10-20 degree variations for the bond angles and is free for the dihedral angles. To outline the alanine optimization results, the structure optimization performed here as a test case is a high-dimensional problem, thus, the VBO method that tries to optimize all the variables x and z converges slowly. Due to the same reason, methods MMDBO and Dropout also underperform in terms of convergence for the alanine problem. Similarly to SADCBO, these two baselines operate variable selection, although using a different selection criterion. However, controlling the selected variable comes at a cost. On the opposite, it turns out that from Figure S2 (fifth row, middle panel), SADCBO virtually never switches to phase II for the Molecular Shape example. Therefore, SADCBO does perform contextual variable selection, but does not control them, it only chooses which of these variables will be included in the surrogate, hence behaving like CBO, but with a variable selection step. This explains why 1) CBO closely follows SADCBO for this example and 2) why other variable selection baselines like MMDBO and Dropout end up far from SADCBO. Interestingly, in this case, the simplified case of optimizing only the design variables x (CUBO) also performs well. This is because our domain experts made good initial choices on the relevant design variables x and the search spaces of context variables z . This type of pre-analysis is time-consuming and more challenging for larger molecules. Hence, a future line of work is to test context-aware BO more comprehensively in molecule structure optimization tasks.

Robot Pushing Task This task was first introduced in Wang et al. [2017], and consists of a control parameter tuning problem for robot pushing. This real-world function returns the distance between a designated goal location and two objects being pushed by two robot hands, whose trajectory is determined by 14 parameters specifying the location, rotation, velocity and moving direction, among others. The function is implemented with a physics engine, the Box2D simulator. There are 6 design variables and 8 contextual variables.

E.2 SYNTHETIC TEST FUNCTIONS

Hartmann-6D function:

$$f(\mathbf{v}) = - \sum_{i=1}^4 \alpha_i \exp \left(- \sum_{j=1}^6 A_{ij}(v^{(j)} - P_{ij}) \right)$$

$$\alpha = (1.0, 1.2, 3.0, 3.2)^T$$

$$\mathbf{A} = \begin{pmatrix} 10 & 3 & 17 & 3.5 & 1.7 & 8 \\ 0.05 & 10 & 17 & 0.1 & 8 & 14 \\ 3 & 3.5 & 1.7 & 10 & 17 & 8 \\ 17 & 8 & 0.05 & 10 & 0.1 & 14 \end{pmatrix}$$

$$\mathbf{P} = 10^{-4} \begin{pmatrix} 1312 & 1696 & 5569 & 124 & 8283 & 5886 \\ 2329 & 4135 & 8307 & 3736 & 1004 & 9991 \\ 2348 & 1451 & 3522 & 2883 & 3047 & 6650 \\ 4047 & 8828 & 8732 & 5743 & 1091 & 381 \end{pmatrix}$$

defined over $\mathcal{V} = [0, 1]^6$. The second, fifth, and sixth variables were considered as design variables, while the first, third, and fourth variables were considered as contextual variables. 6 noise variables were added. Table S1 provides the results of a Sobol global sensitivity analysis performed using evaluations of the function collected over a grid of $N = 917504$ samples [Sobol, 2001]. Adding up the first order indices for design and contextual variables separately leads to $S_x \approx 0.124$ and $S_z \approx 0.196$. This means that with respect to first-order interactions, contextual variables have more impact than design variables, in this synthetic example. One should notice however that these indices are computed across the whole search space and not specifically at the optimum.

Table S1: Sobol global sensitivity analysis for the Hartmann-6D function using $N = 917504$ samples.

Variable	First order sensitivity indices	Total order sensitivity indices
$z^{(1)}$	0.107	0.343
$x^{(2)}$	0.006	0.399
$z^{(3)}$	0.007	0.052
$z^{(4)}$	0.082	0.379
$x^{(5)}$	0.106	0.297
$x^{(6)}$	0.012	0.482

Hartmann-4D function:

$$f(\mathbf{v}) = \frac{1}{0.839} \left(1.1 - \sum_{i=1}^4 \alpha_i \exp \left(- \sum_{j=1}^4 A_{ij}(v^{(j)} - P_{ij}) \right) \right)$$

$$\alpha = (1.0, 1.2, 3.0, 3.2)^T$$

$$\mathbf{A} = \begin{pmatrix} 10 & 3 & 17 & 3.5 \\ 0.05 & 10 & 17 & 0.1 \\ 3 & 3.5 & 1.7 & 10 \\ 17 & 8 & 0.05 & 10 \end{pmatrix}$$

$$\mathbf{P} = 10^{-4} \begin{pmatrix} 1312 & 1696 & 5569 & 124 \\ 2329 & 4135 & 8307 & 3736 \\ 2348 & 1451 & 3522 & 2883 \\ 4047 & 8828 & 8732 & 5743 \end{pmatrix}$$

defined over $\mathcal{V} = [0, 1]^4$. The first and fourth variables were considered as design variables, while the second and third variables were considered as contextual variables. 3 noise variables were added. Table S2 provides the results of a Sobol

global sensitivity analysis performed using evaluations of the function collected over a grid of $N = 300000$ samples. Adding up the first order indices for design and contextual variables separately leads to $S_x \approx 0.579$ and $S_z \approx 0.091$. This means that with respect to first-order interactions, design variables have much more impact on the output than contextual variables. The gap slightly reduces when considering total order sensitivity indices. However, it is worth remembering that these indices are computed across the whole search space and not specifically at the optimum.

828
829
830
831
832

Table S2: Sobol global sensitivity analysis for the Hartmann-4D function using $N = 300000$ samples.

Variable	First order sensitivity indices	Total order sensitivity indices
$x^{(1)}$	0.307	0.477
$z^{(2)}$	0.037	0.279
$z^{(3)}$	0.054	0.103
$x^{(4)}$	0.272	0.526

Ackley 5D function:

$$f(\mathbf{v}) = -20 \exp \left(-0.2 \sqrt{\frac{1}{5} \sum_{j=1}^5 (v^{(j)})^2} \right) - \exp \left(\frac{1}{5} \sum_{j=1}^5 \cos(2\pi v^{(j)}) \right) + 20 + e^1$$

defined over $\mathcal{V} = [-5, 5]^5$. 8 noise variables were added.

833

EggHolder 2D function:

$$f(\mathbf{v}) = -(v^{(2)} + 47) \sin \left(\sqrt{\left| v^{(2)} + \frac{v^{(1)}}{2} + 47 \right|} \right) - v^{(1)} \sin \left(\sqrt{|v^{(1)} - (v^{(2)} + 47)|} \right)$$

defined over $\mathcal{V} = [-512, 512]^2$. The first variable was considered as a design variable, and the second one as a contextual variable. 4 noise variables were added. A Sobol global sensitivity analysis performed using evaluations of the function collected over a grid of $N = 3000000$ samples shows that both variables have a similar contribution to the output (Table S3).

834
835
836

Table S3: Sobol global sensitivity analysis for the EggHolder-2D function using $N = 3000000$ samples.

Variable	First order sensitivity indices	Total order sensitivity indices
$x^{(1)}$	0.001	0.998
$z^{(2)}$	0.0004	0.999